Journal of World Architecture, 2025, Volume 9, Issue 3
https://ojs.bbwpublisher.com/index.php/JWA
Online ISSN: 2208-3499
Print ISSN: 2208-3480

Finite Element Simulation of Mid-Joints in Chuandou-Style Tenon-Mortise Connections of Dong Drum Towers in Guizhou Based on ABAQUS

Ziquan Jiang, Shuang Pu*, Chuanteng Huang, Jilun Cai, Junxiu Liu, Hongyao Tang

School of Engineering, Zunyi Normal University, Zunyi, China

**Author to whom correspondence should be addressed.*

***A*bstract:** As iconic structures in Dong ethnic villages of Guizhou, drum towers hold significant cultural and architectural value. However, research on their mechanical behavior, particularly the mechanical performance of their joints, remains limited, with numerical simulation studies lagging behind theoretical and experimental investigations. This study first establishes an orthotropic elastoplastic constitutive model for timber based on experimental data from Chuandou-style timber structures, determining key parameters such as elastic modulus, shear strength, and plastic strain.Subsequently, a refined finite element model was established using ABAQUS, and its reliability was validated through comparative analysis of stress nephograms, skeleton curves, and other key outcomes with experimental data. The findings provide valuable references for engineering design.

Keywords: Chuandou-style timber structure; Mid-joints in tenon-mortise connections; numerical simulation; ABAQUS

Online publication: June 30, 2025

1. Introduction

As a cultural symbol and core tourism resource in Guizhou Province, the Dong drum towers' structural safety directly relies on the mechanical performance of their Chuandou-style tenon-mortise joints. Existing drum towers commonly exhibit structural deterioration, such as cracking of surrounding beams and column base erosion (**Figure 1**), while newly constructed towers have experienced wind-induced collapse accidents due to structural instability.

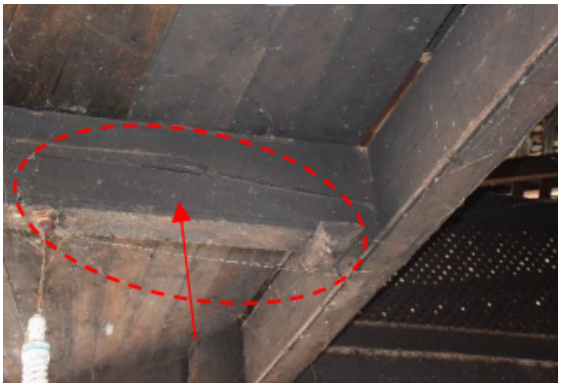

(a) Cracking of surrounding beams

(b) Biological degradation at column bases

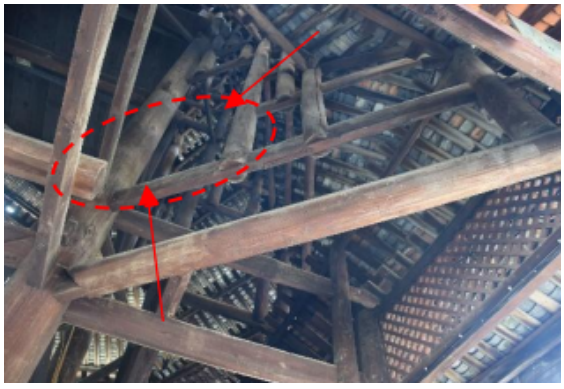

(c) Cracking of short columns and drainage beams

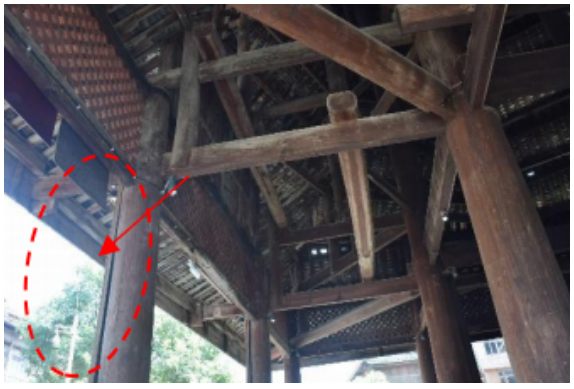

(d) Cracking of eaves columns

Figure 1. Pathological phenomena in timber structures of dong ethnic historic architecture

Research on Dong ethnic historic architecture has predominantly focused on architectural and ethnological disciplines in China, while specialized international studies remain notably absent. In terms of artistic value, scholars have dissected the aesthetic significance of drum towers through perspectives such as artistic features, cultural connotations, and decorative totems [1–3]. Cultural semiotic studies further unveil their multifunctional role as carriers of ethnic culture, proposing a "culture-time-space" tripartite framework to conceptualize their spatial essence [4–6]. Significant breakthroughs have been achieved in research on traditional construction techniques: a classification system for drum towers has been established through typological methods, while modular design principles have been integrated to develop modern adaptive pathways for preserving and evolving these craftsmanship traditions [7–9]. The research team in mathematical theory has pioneered the revelation of inherent mathematical regularities in drum towers through geometric configuration and structural logic [10–12]. In the field of structural engineering, research remains in its nascent stage. Scholars have employed finite element simulations to elucidate the energy dissipation mechanisms and stiffness degradation patterns of tenon-mortise joints [13–15].

Furthermore, an orthotropic constitutive model for timber has been established, laying the foundation for seismic performance studies of wooden frameworks [16–18]. Current research exhibits critical limitations in numerical simulations and the mechanical mechanisms of joints, necessitating urgent systematic structural analyses. This study investigates the stress transfer mechanisms of refined mid-joints in Chuandou-style timber frames under static and dynamic loads, grounded in their structural characteristics. By establishing a detailed

mechanical model of the tenon-mortise connections, the research elucidates load-path interactions and nonlinear response patterns, thereby providing a theoretical foundation for assessing the overall stability of drum towers and optimizing restoration techniques. The study is designed to achieve dual objectives: safeguarding the structural safety of Dong village residents and perpetuating the intangible cultural heritage (ICH) of traditional timber construction techniques, while concurrently advancing the sustainable development of ethnic tourism economies. These goals align with China's national strategy for low-carbon architectural development.

2. Finite element simulation of mid-joints in Chuandou-style tenon-mortise connections

This section presents the development of a refined finite element analysis model in ABAQUS, grounded in experimental studies on mid-joints in tenon-mortise connections within Chuandou-style timber structures conducted by Li [19].

The test specimen, as illustrated in **Figure 2(a)**, consists of a column with a height of 1325 mm and a diameter of 200 mm, and a transverse beam (Chuanfang beam) measuring 1950 mm in length, 85 mm in width, and 190 mm in height. The column base was fixed during testing, and loads were applied via hydraulic jacks positioned 550 mm left and 1100 mm right from the column center, as depicted in the loading configuration shown in **Figure 2(b)**.

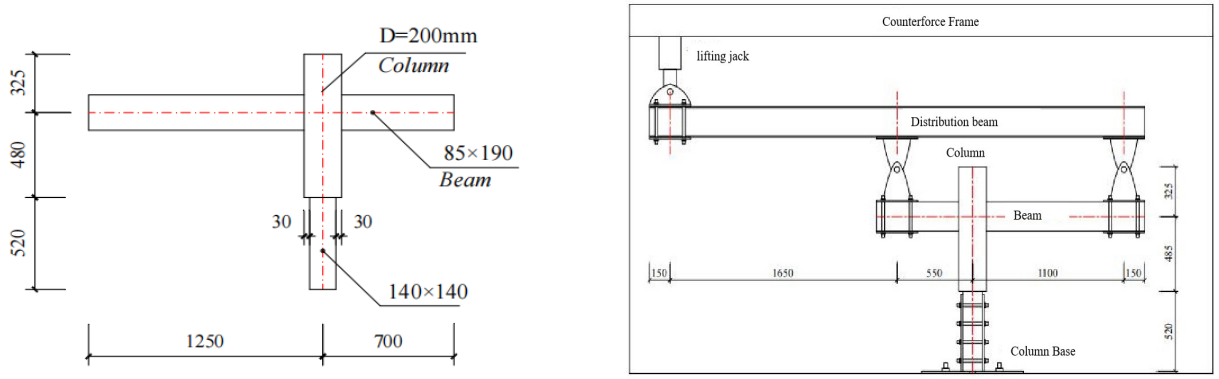

(a) Test specimen model

(b) Specimen loading configuration diagram

Figure 2. Refined finite element analysis model in test

The material parameters of Chinese fir timber used for establishing the finite element model are summarized in **Table 1**, as compiled from material property tests conducted by Li [19].

Table 1. Material parameters of Chinese fir timber

Modulus(MPa)		Poisson's ratio		Strength (MPa)		Shear strength (MPa)		Fracture energy (MPa)	
E_L	12160	V_{LR}	0.3	σ_{Lt}	79.00	S_{LR}	4.5	G_{fL}	19653
E_R	1400			σ_{Lc}	48.84				
E_T	700	V_{RT}	0.3	σ_{Rt}	4.0	S_{RT}	2.0	G_{fR}	231.8
G_{LR}	912			σ_{Rc}	5.0				
G_{RT}	218.9	V_{LT}	0.5	σ_{Tt}	4.0	S_{LT}	5.0	G_{fT}	231.8
G_{LR}	729.6			σ_{Tc}	5.0				

As illustrated in **Figure 3**, the finite element analysis model of mid-joints in Chuandou-style tenon-mortise connections is presented, with the modeling procedure systematically summarized as follows:

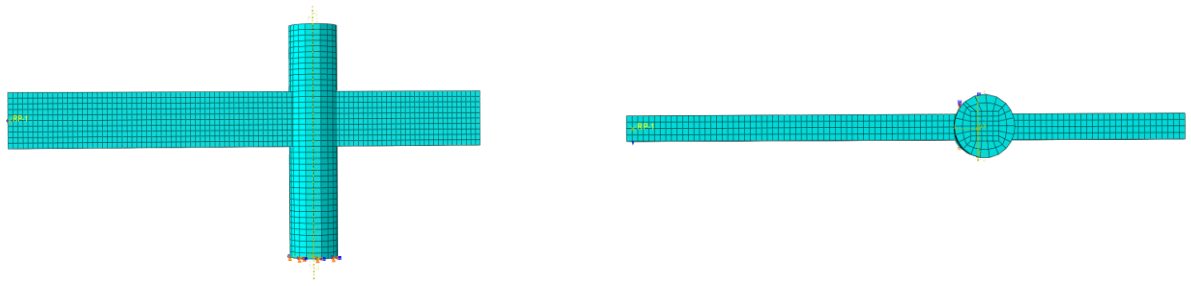

(a) Comprehensive finite element model (b) Structural characteristics of Chuandou-style Tenon-Mortise Joints

Figure 3. The finite element model of mid-joints in Chuandou-style tenon-mortise connections

(1) Element selection and mesh generation: The transverse beams and mortised columns were modeled using three-dimensional solid elements (C3D8R). The cylindrical geometry at the mortise region was partitioned, and refined meshing was applied to the hollowed section. At the tenon sides where the load-bearing cross-section diminishes, the element size is strictly controlled to less than half of the narrow-edge width, while a nominal mesh width of 20 mm is adopted in bulk regions to ensure computational accuracy.

(2) Operational definition of contact: The normal behavior was defined as hard contact with separation permitted, utilizing the default constraint enforcement formulation; the tangential behavior adopted a penalty friction formulation with an isotropic friction coefficient of 0.4.

(3) Contact interaction establishment: For zero-clearance conditions, surface-to-surface contact pairs were generated through contact pair detection, where the column interface was designated as the master surface and the transverse beam interface as the slave surface. For models with initial gaps, the same surface-to-surface contact formulation was retained, preserving the original master-slave assignments and interaction properties identical to those of the gapless configuration.

(4) Boundary condition configuration: In accordance with the experimental setup conducted by Li, where the lower portion of the column base was intentionally weakened and fixed, the finite element model was configured to simulate a hinged connection at the interface between the upper and lower segments of the column [19]. The modeling process initiated from this hinged section. The column base was idealized as a pinned connection by constraining translational degrees of freedom (U1, U2, U3) and rotational degrees of freedom about the X- and Z-axes (UR1, UR3) to zero, while retaining rotational freedom about the Y-axis (UR2). A tabular amplitude definition was employed, with the amplitude fixed at unity and time-frequency incrementation applied throughout the analysis.

(5) Load application methods:

(a) Monotonic static loading: A rotational amplitude was imposed through boundary condition configuration to simulate continuous rotational displacement loading ranging from 0 to 0.18 rad, achieving kinematic equivalence with experimental hydraulic jack loading protocols.

(b) Cyclic loading protocol: Cyclic loading was applied following the displacement-controlled method outlined in Li's study, utilizing the rotational angle-vertical displacement relationship $y=1250\tan\theta$ as the governing criterion [19]. The multi-stage loading protocol comprised: single-cycle phase: 0.03–0.05 rad angular displacement range; three-cycle phase: 0.07–0.13 rad angular displacement range with

cumulative loading executed across 15 cycles.

The amplitude-time curve was rigorously aligned with experimental quasi-static test data, ensuring kinematic equivalence in hysteresis response.

3. Analysis of results

3.1. Analysis of monotonic static loading results

As illustrated in **Figure 4(a),** localized compressive deformation is evident beneath the mortise, which aligns with the experimental observations in **Figure 4(b)**. This phenomenon arises from the abrupt increase in interfacial stiffness at the contact zone between the transverse beam and mortise during the continuous downward loading imposed by the hydraulic jack, ultimately inducing significant compressive strains on the mortise underside.

(a) Finite element analysis results (b) Experimental results

Figure 4. Comparative analysis of mortise deformation under monotonic loading conditions

As shown in **Figure 5**, both experimental and finite element simulation results demonstrate concave deformation at the contact interface between the transverse beam and the mortise. This deformation is attributed to the progressive downward compression of the transverse beam against the column during contact interaction, inducing localized plastic strain accumulation in the mortise region.

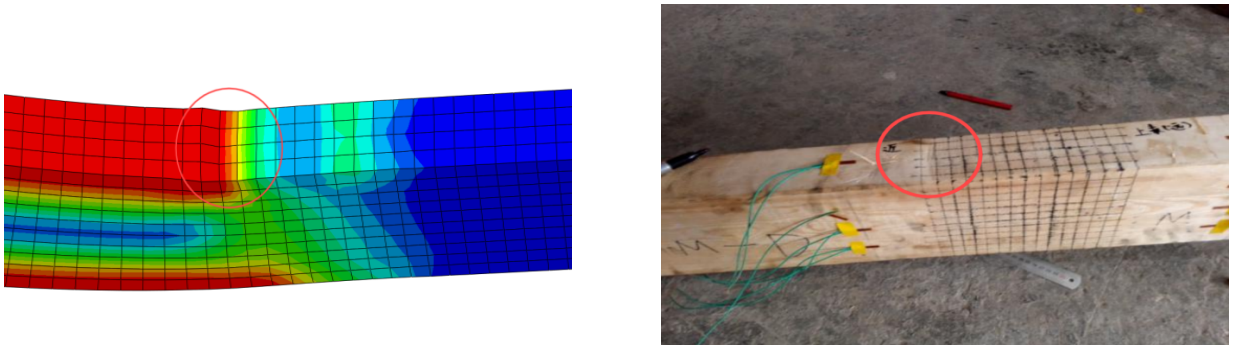

(a) Finite element analysis results (b) Experimental results

Figure 5. Comparative analysis of transverse beam deformation under monotonic loading conditions

As depicted in **Figure 6**, the experimental and finite element analysis (FEA) load-displacement curves exhibit consistent trends (discrepancy ≤ 10%), subdivided into two distinct phases: slip-stiffening and slip-plateau. During the initial loading phase, rotational slippage of the transverse beam was induced by negligible force input. Following contact with the mortise-column interface, the system transitioned into a stiffness ascent phase characterized by progressive geometric interlock hardening, which was succeeded by gradual stiffness degradation until eventual stabilization due to orthotropic plasticity saturation in the mortise region.

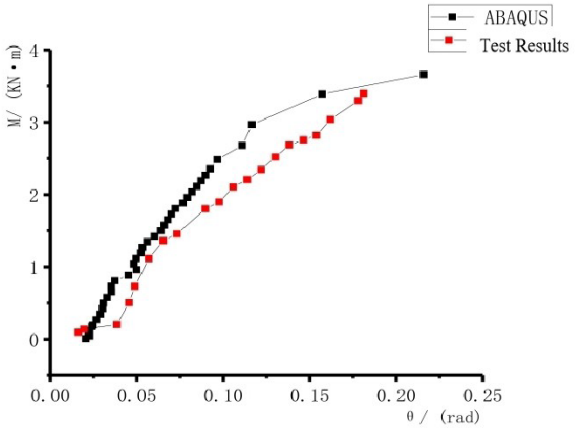

Figure 6. $M-\theta$ Curve of monotonic loading

3.2. Analysis of cyclic loading results

As illustrated in **Figure 7**, both simulation results and experimental data exhibit significant compressive deformation at the upper mortise region, while the deformation magnitude in the lower mortise region remains comparatively minor. This observation aligns with the experimental measurements, confirming consistent deformation patterns across numerical and physical models.

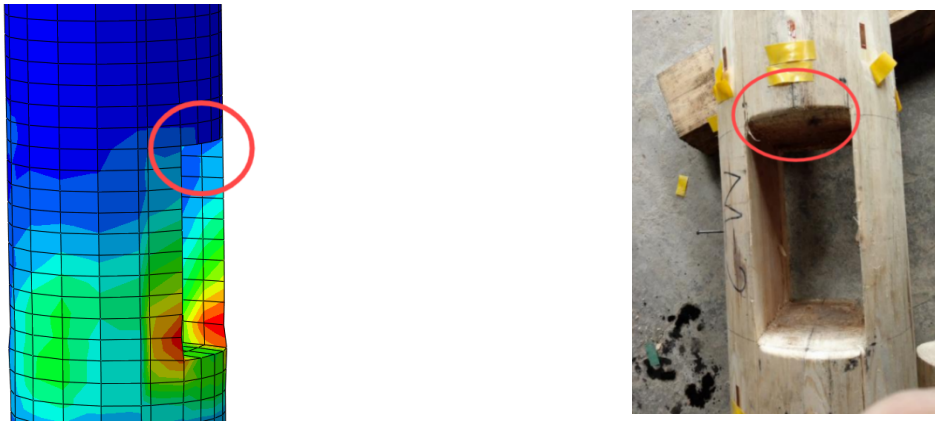

(a) Finite element analysis results (b) Experimental results

Figure 7. Deformation comparison of mortise-column interface in cyclic loading test

As illustrated in **Figure 8**, pronounced compressive deformation is observed at the contact interface between the transverse beam and mortise in the Chuandou-style mortise-tenon joint. Notably, the longer segment of the transverse beam exhibits greater compressive deformation magnitudes, demonstrating close alignment with

experimental measurements. This consistency validates the numerical model's capability to capture localized orthotropic plasticity and stress redistribution mechanisms inherent to traditional timber connections.

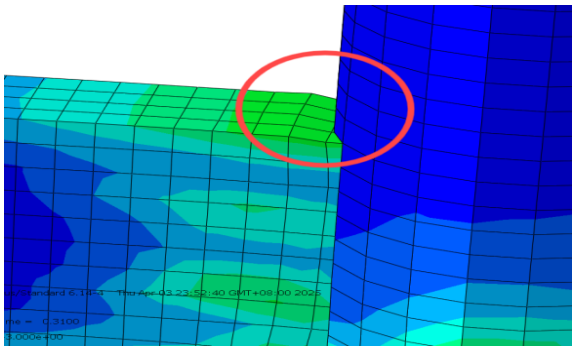

(a) Finite element analysis results 1

(b) Experimental results 1

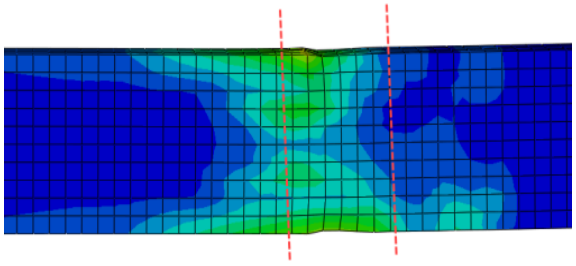

(c) Finite element analysis results 2

(d) Experimental results 2

Figure 8. Deformation comparison of transverse beams in cyclic loading tests

As shown in **Figure 9**, the stress exerted on the through-tenon beam in the parallel-to-grain direction has not yet reached its critical yield stress, and its mechanical behavior exhibits significant differences compared to that of variable-section straight tenon joints.

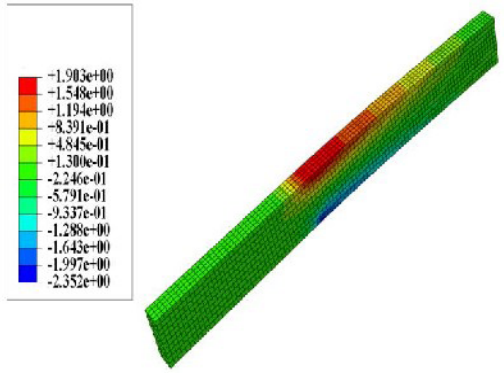

(a) Stress nephograms along the grain direction

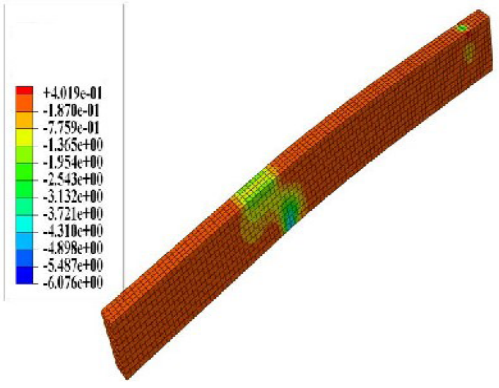

(b) Stress nephograms perpendicular to grain

Figure 9. Stress nephograms of through-tenon beam

This phenomenon indicates that, under a constant cross-sectional configuration of the tenon, the stress in the parallel-to-grain direction remains relatively low, primarily attributed to the absence of compressive loading on the through-tenon beam along this orientation. In contrast, significant yielding is observed in the perpendicular-to-grain direction of the FEA model, indicating that this region has likely entered the plastic deformation regime. The observed stress distribution pattern exhibits a high degree of consistency with variable-section straight tenon joints, a characteristic that strongly reflects the quintessential mechanical behavior inherent to traditional straight tenon joints.

As shown in **Figure 10**, the Chuandou-style mortise-tenon joint column exhibits fundamentally analogous global stress distribution patterns in both longitudinal and transverse grain directions. However, a pronounced cross-sectional reduction is observed in the longitudinal grain direction, accompanied by significantly higher stresses at the mortise openings compared to the transverse grain direction.

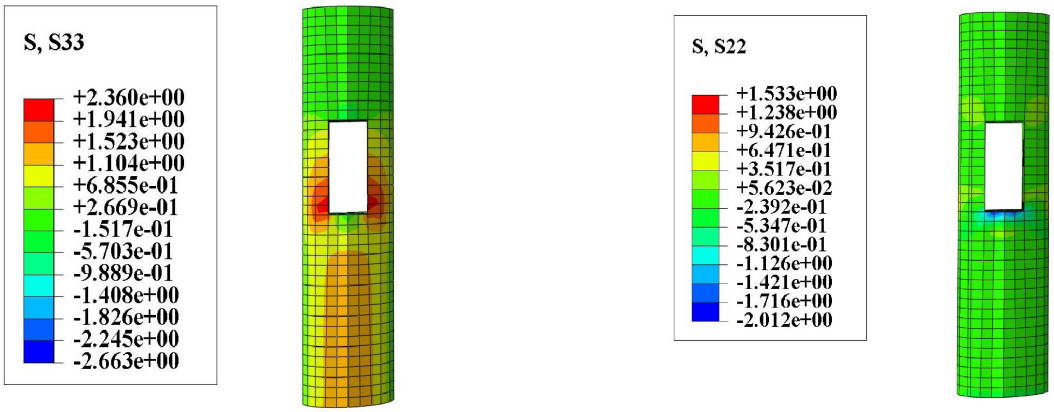

(a) Stress nephograms along the grain direction (b) Stress nephograms perpendicular to grain

Figure 10. Stress nephograms of column

As illustrated in **Figure 11**, the skeleton curves of the mortise-tenon joint specimens derived from finite element simulations and experimental literature data exhibit a consistent trend: the bending moment progressively increases with rotational angle.

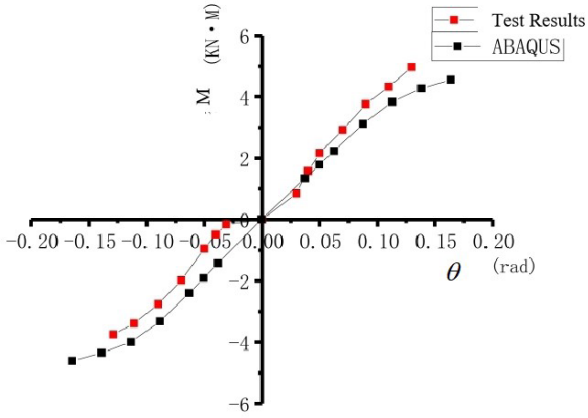

Figure 11. Skeleton curve

Both numerical and experimental results demonstrate analogous behavioral patterns, with an error margin not exceeding 5%. The observed deviations primarily arise from interfacial contact imperfections in experimental joints that fail to achieve the idealized tightness simulated numerically. Fabrication-induced variations during manufacturing processes result in corresponding minor discrepancies in the experimental results.

4. Conclusion

This study presents a refined finite element modelling process for Chuandou-style timber mortise-tenon joints using ABAQUS. The mechanical behaviour of mortise openings and cross beams under both monotonic and cyclic loading was systematically investigated, with emphasis on stress distribution patterns and skeleton curves. The results validate the reliability of the proposed refined finite element model in simulating joint mechanics. The research findings and methodologies can be directly applied to engineering design practices. Furthermore, this framework facilitates subsequent parametric studies to investigate the influence of critical design parameters, such as column diameter, interfacial gap size, and crossbeam width, on the mechanical performance of mortise-tenon joints.

Funding

Science and Technology Planning Project of Zunyi City of China (Project No.: Zun Shi Ke He HZ Zi [2022] 121), College Students' Innovation and Entrepreneurship Training Program (Project No.: 202310664031), Guizhou Provincial First-Class Undergraduate Major "Civil Engineering" (Project No.: Qian Jiao Han [2022] No. 61), Guizhou Provincial First-Class Course Construction Project (Project No.: 2022JKXX0165, 2024JKXN0064)

Disclosure statement

The authors declare no conflict of interest.

References

[1] Liu Y, 2010, Artistic Study of Dong Ethnic Drum Towers, thesis, Guangxi University for Nationalities.

[2] Gao B, 2013, An Anthropological Study of the Artistic World of Dong Drum Towers, thesis, Guangxi University for Nationalities.

[3] Tian X, 2016, Architectural Art of Dong Drum Towers in Southeastern Guizhou, thesis, Guizhou Normal University.

[4] Liu J, 2011, On the Aesthetic Value of Dong Drum Tower Architecture. Art Education Research, 2011: 25.

[5] Liu F, 2012, Construction Techniques and Cultural Significance of Drum Towers in Zhaoqing Dong Community, thesis, Chinese National Academy of Arts.

[6] Xiao J, 2015, Cultural Spatial Connotations of Dong Drum Towers. Journal of Huaihua University, 2015: 6–8.

[7] Liao J, 2007, A Study on the Traditional Cultural Characteristics of the Southern Dong Ethnic Group. Ethnic Publishing House, China.

[8] Ren S, Cheng D, Liang Z, 2008, Architectural Landscapes and Cultural Connotations of Dong Villages. Guangxi Urban Construction, 2008: 36–39.

[9] Wu H, 2010, Cultural Connotations and Social Functions of Dong Drum Towers. Forum on Education and Culture,

2010: 73–77.

[10] Luo Y, 2013, Perspectives on Dong Mathematical Culture. Journal of Mathematics Education, 2013: 67–72.

[11] Zhang H, Luo Y, 2011, Mathematical Culture in Dong Drum Tower Architecture. Journal of Kaili University, 2011: 189.

[12] Wu X, Zhang H, 2020, Investigation of Mathematical Elements in Dong Architecture. Journal of Kaili University, 2020: 1–5.

[13] Qin S, Yang N, Hu H, Zhang L, 2018, Dynamic Characteristics of Damaged Ming–Qing Timber Structures. Journal of Building Structures, 2018: 130–137.

[14] Dong J, Xue J, Sui Y, Xia H, 2019, Hysteretic Behavior and Damage Assessment of Asymmetric Mortise–Tenon Joints in Ancient Timber Structures Under Varying Looseness. Chinese Journal of Applied Mechanics, 2019: 1321–1327, 1519.

[15] Yang N, Tan S, Qin S, 2019, Seismic Vulnerability Analysis of Damaged Ancient Timber Structures. World Earthquake Engineering, 2019: 95–104.

[16] Li Q, 2008, Mechanical Properties and Seismic Resistance of Mortise–Tenon Joints and Timber Frames in Ancient Architecture, thesis, Xi'an University of Architecture and Technology.

[17] Dong C, 2010, Mechanical Behavior and Experimental Study of Mortise–Tenon Connections in Ancient Timber Structures, thesis, Xi'an University of Architecture and Technology.

[18] Sui Y, Zhao H, Xue J, Zhang H, Xie Q, 2010, Experimental Study on Straight Tenon and Dovetail Joints in Ancient Timber Structures. World Earthquake Engineering, 2010: 88–92.

[19] Li P, 2016, Experimental Study on the Seismic Performance of Mortise–Tenon Connections in Chuandou-Style Timber Structures, thesis, Chongqing University.